Precise Supramolecular Control of Selectivity in the Rh-Catalyzed Hydroformylation of Terminal and Internal Alkenes

Paweł Dydio,[†] Remko J. Detz,[†,‡] and Joost N. H. Reek*,[†]

[†]van't Hoff Institute for Molecular Sciences, University of Amsterdam, Science Park 904, 1098 XH, Amsterdam, The Netherlands
[‡]InCatT B.V., Science Park 904, 1098 XH, Amsterdam, The Netherlands

S *Supporting Information*

ABSTRACT: In this study, we report a series of DIMPhos ligands **L1−L3**, bidentate phosphorus ligands equipped with an integral anion binding site (the DIM pocket). Coordination studies show that these ligands bind to a rhodium center in a bidentate fashion. Experiments under hydroformylation conditions confirm the formation of the mononuclear hydridobiscarbonyl rhodium complexes that are generally assumed to be active in hydroformylation. The metal complexes formed still strongly bind the anionic species in the binding site of the ligand, without affecting the metal coordination sphere. These bifunctional properties of DIMPhos are further demonstrated by the crystal structure of the rhodium complex with acetate anion bound in the binding site of the ligand. The catalytic studies demonstrate that substrate preorganization by binding in the DIM pocket of the ligand results in unprecedented selectivities in hydroformylation of terminal and internal alkenes functionalized with an anionic group. Remarkably, the selectivity controlling anionic group can be even 10 bonds away from the reactive double bond, demonstrating the potential of this supramolecular approach. Control experiments confirm the crucial role of the anion binding for the selectivity. DFT studies on the decisive intermediates reveal that the anion binding in the DIM pocket restricts the rotational freedom of the reactive double bound. As a consequence, the pathway to the undesired product is strongly hindered, whereas that for the desired product is lowered in energy. Detailed kinetic studies, together with the in situ spectroscopic measurements and isotope-labeling studies, support this mode of operation and reveal that these supramolecular systems follow enzymatic-type Michaelis−Menten kinetics, with competitive product inhibition.
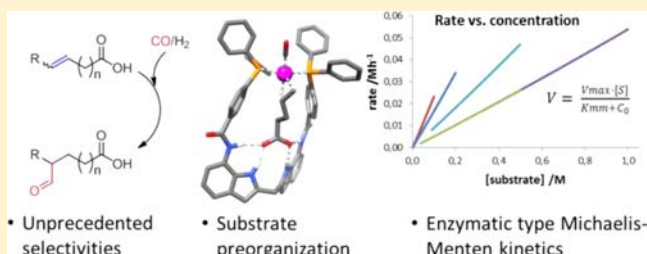
INTRODUCTION

Transition metal catalysis is a powerful enabling technology for the sustainable preparation of chemical compounds.[1] However, the value of the individual catalytic transformations depends largely on the access to catalysts displaying the required selectivity, activity, and stability.[2] Various tools to control these decisive features by modification of ligands coordinated to the catalytically active metal centers have been introduced.[3] The traditional approach to catalyst development involves knowledge-supported trial-and-error protocols, for which combinatorial and high-throughput screening methods of putative catalysts have demonstrated their added value.[4] If the required selectivity is not obtained using these strategies, "directing groups" (DGs) can be used. Such groups should be introduced to the substrate molecules, and during the reaction they steer the selectivity by coordination to the metal center, directing the reaction toward the desired product.[5] Although effective, this method is limited to substrates with DGs spatially close to the reactive functionality, imposing limitations. Moreover, the reaction occurring at the metal center should be compatible with the DGs, further limiting its potential. For these reasons, it is highly interesting to develop alternative methodologies with directing groups that operate via interactions between the functional groups of the substrate and the ligand of the catalyst.

This can be achieved by using bifunctional ligands that can coordinate to the metal center and bind noncovalently to a substrate molecule.[6] This supramolecular substrate binding can in principle preorganize the reactive functionality at the catalytic center (Figure 1) such that one of the competitive reaction pathways is favored over the competing ones,
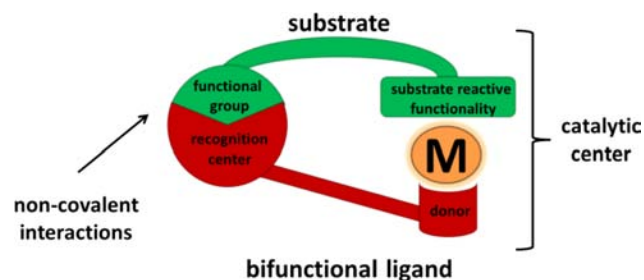

Figure 1. General concept of substrate preorganization by a catalyst with a bifunctional ligand, consisting of a donating function for catalytic center coordination and a specific recognition site for binding to a functional group of a substrate.

controlling the overall selectivity. This principle was demonstrated in selective oxidation reactions catalyzed by metalloporphyrins by Breslow and co-workers,[7] using hydrophobic or coordination interactions as the driving force. Hydrogen bonding is highly directional and can lead to relatively strong interactions; hence, it provides a powerful tool for the rational design of selective catalysts that operate via substrate orientation.[8] As such, it was elegantly used for controlling the regioselectivity in the Ru-catalyzed hydration of alkynes,[9] the Mn-catalyzed C−H oxidation at sp[3]-carbon atoms,[10] and the Rh-catalyzed hydroformylation of β,γ-unsaturated carboxylic acids.[11] A two-point hydrogen-bonding interaction allowed one also to control regio- and enantioselectivity in the Ru-catalyzed epoxidation of olefinic double bonds,[12] and a simple single hydrogen bond was shown to improve the selectivity in the Co-catalyzed cyclopropanation[13] and the enantioselectivity in the Rh-catalyzed hydrogenation of olefins.[14]

The examples reported so far[9−14] addressed successfully quite small or rigid substrate molecules of rather limited scope. We anticipated that the "remote control" for more flexible and bigger substrates requires catalytic systems based on well-defined, rigid complex structures, in which the positions of the controlling unit and the catalytic centers are precisely defined. In this respect, the use of functionalized bidentate ligands has an advantage over functionalized monodentate ligands[11] as the number of possible complexes that can be formed is significantly lower. We considered that neutral anion receptors[15] that operate with hydrogen bonding are excellent candidates for the substrate-directing motifs for supramolecular catalysts, as they can interact with one of the most common functional groups in organic compounds, that is, carboxyl moiety. Therefore, we chose the 7,7′-diamido-2,2′-diindolylmethane (the DIM pocket),[16] a tailor-made receptor for carboxylate and phosphate anions, as a scaffold to prepare new bidentate DIMPhos ligands L1−L3 (Figure 2). In this Article, we report in depth studies that demonstrate that these new ligands can control the regioselectivity in hydroformylation of alkenes by substrate orientation in the binding site. Especially, control over selectivity in the hydroformylation of internal alkenes is challenging,[17] and there are only a few literature

precedents of precise selectivity control.[11,18,19] DFT calculations of the decisive intermediates reveal the mode of operation of this new catalyst. The anion binding in the DIM pocket restricts the rotational freedom of the reactive double bound required during the hydride migration step. As a result, the pathway to the undesired product is strongly hindered, whereas that for the desired product is lowered in energy. The kinetic studies and the in situ spectroscopic measurements support this mechanism, and reveal that the system follows Michaelis−Menten kinetics. Full details of these studies are presented in the following sections of this Article.[20]

■ RESULTS AND DISCUSSION

Coordination and Anion Binding Properties. We first investigated the anion binding and coordination properties of the DIMPhos ligands. Strong anion binding of **L1** was apparent as the presence of acetate anions triggered a significant downfield shift of the NH signals ($\Delta\delta$ = 2.4−3.9 ppm) in the ^{1}H NMR spectra in CD_2Cl_2. Further, the titration studies revealed the high association constant, $K_a \gg 10^5$ M^{-1}, for the formation of a 1:1 ligand−acetate anion complex. Upon the addition of the rhodium precursor, $[\text{Rh(acac)}(C_2H_4)_2]$ (acac = acetylacetonate), the rhodium−ligand complex, the precursor of the active hydroformylation catalyst[17a] with the acetate remained bound in the DIM pocket, $[\text{Rh}(\textbf{L1}\cdot\text{AcO})(\text{acac})]$, was formed. Also, the addition of $[\text{RhCl(CO)}_2]_2$ as metal precursor led to the formation of the complex with both phosphorus atoms coordinated to the rhodium center in a trans mutual orientation, with the acetate anion bound in the DIM pocket. The structure of this complex was also elucidated by the X-ray crystallography of TBA$[\text{Rh}(\textbf{L1}\cdot\text{AcO})(\text{CO})(\text{Cl})]$ crystals (Figure 2 (right), TBA$^+$ = tetrabutylammonium cation).[20a] As anticipated, the acetate is bound in the binding site with four strong hydrogen bonds (the N−O distances are 2.737(3) and 3.006(3) Å, for the amide and indole N atoms, respectively), and, importantly, its aliphatic group points toward the metal center.

High-pressure (HP) NMR studies reveal that a 1:1 mixture of ligand **L1** and $[\text{Rh(acac)(CO)}_2]$ under hydroformylation conditions, 5 bar CO/H$_2$ (1:1), results in exclusive formation of a trigonal bipyramidal hydrido complex $[\text{Rh}(\textbf{L1})(\text{CO})_2\text{H}]$, the catalytically active complex for hydroformylation.[17] A doublet of triplets for the hydride signal at δ = −9.5 ppm in the ^{1}H NMR spectrum indicates that the hydride couples both with rhodium and the two phosphorus donor atoms. This signal simplifies in a phosphorus-decoupled ^{1}H{^{31}P} NMR experiment, and the observed doublet is consistent with the hydride coupled to rhodium. The ^{31}P{^{1}H} NMR spectrum displays only one doublet at δ = 36.7 ppm, indicative of the phosphine coupling with rhodium and showing the equivalency of both phosphorus atoms. Upon lowering the temperature from 25 to −95 °C, the signals in both ^{1}H and ^{31}P NMR spectra broaden and split into two sets.[21] These experiments establish that the bidentate ligand **L1** coordinates in both equatorial−equatorial (eq−eq) and equatorial−axial (eq−ax) fashion and that at room temperature these isomeric complexes are in fast equilibrium on the NMR time scale. The low value of the phosphorus−hydride coupling (4.0 Hz) indicates that the eq−eq isomer dominates the equilibrium.[22] In line with this, high-pressure infrared (IR) studies using either H$_2$/CO or D$_2$/CO (both 1:1, 20 bar) show absorption bands in the carbonyl region corresponding to both eq−eq and eq−ax isomeric complexes.[23] Furthermore, DFT calculations (BP86, SV(P))
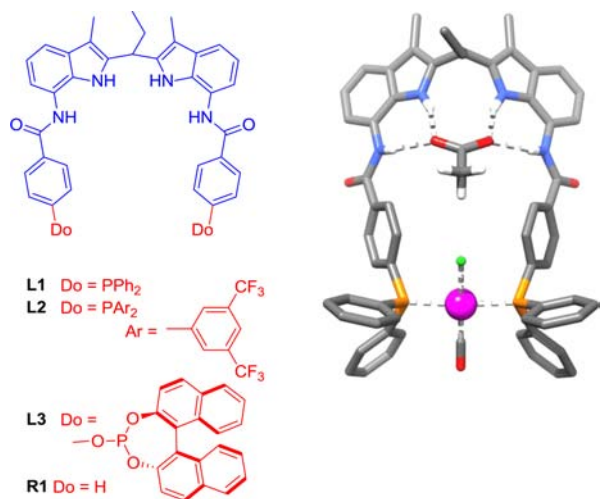

Figure 2. Structure of DIMPhos ligands **L1**−**L3** and DIM anion receptor **R1** (left) and X-ray structure of the supramolecular complex $[\text{Rh}(\textbf{L1}\cdot\text{AcO})(\text{CO})\text{Cl}]^-$ (right); TBA$^+$ counterion, disordered solvent molecules, and most hydrogen atoms are omitted for clarity.

indicate that the complex can adopt both conformations, and that the eq−eq isomer is more favored by 11.4 kJ/mol.[24]

Importantly, HP NMR studies show that the coordination geometry around the rhodium center does not change in the presence of anions (acetate or $H_2PO_4^-$) that are bound in the binding site of the ligand. The signals of the NH groups of the ligand are shifted toward lower fields in the ^{1}H NMR spectra ($\Delta\delta$ = 2.5−3.1 ppm), confirming the formation of strong hydrogen bonds between the anions and the binding site of the ligand.[15] The carbonyl absorption bands of the rhodium complex show only a small shift in the HP IR spectra to lower wavenumbers ($\Delta\nu$ up to 5 cm^{-1}) upon anion binding, indicating a slightly increased electron density at the metal complex. The binding constants for carboxylate and phosphate anions to the DIM binding site of $[Rh(L1)(CO)_2H]$ were determined from titration experiments performed at 5 bar CO/H$_2$ (1:1) in CD$_2$Cl$_2$ by using HP NMR spectroscopy. These studies reveal that only one anion is bound in the DIM pocket of $[Rh(L1)(CO)_2H]$, and that the association constants for CH$_3$COO$^-$ and H$_2$PO$_4^-$ are higher than 10^5 M^{-1} and around $10^{3.7}$ M^{-1}, respectively. In contrast to these anionic species, the acidic (CH$_3$COOH and H$_3$PO$_4$) and the (alkyl) esters analogues are not bound in the DIM pocket of the ligand,[24] and therefore they are well suited for control experiments.

Regioselective Hydroformylation of Terminally Unsaturated Aliphatic Acids. We next studied the performance of ligand **L1** in the rhodium-catalyzed hydroformylation of a series of deprotonated ω-unsaturated carboxylic acids **1a−8a** (Scheme 1), varying the aliphatic chain length between the

Scheme 1
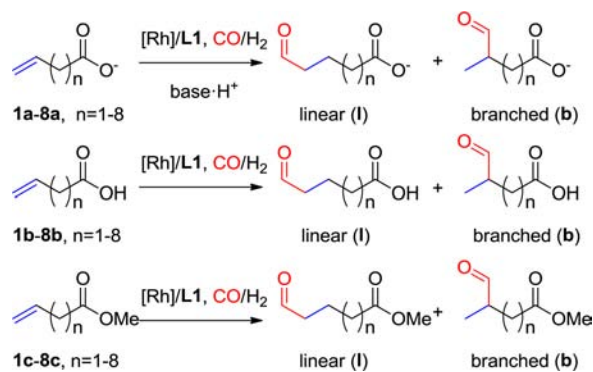
carboxyl moiety and the double bond, that is, from 3-butenoic to 10-undecenoic acid (Table 1). Molecular modeling reveals that the shortest substrate **1a** (3-butenoate anion) cannot simultaneously bind to the anion binding site and coordinate to the Rh center with its double bond. The homologue substrate **2a** that is one carbon longer (4-pentenoate anion) precisely spans the distance between the metal and the binding site of the catalyst, whereas the other substrates **3a−8a** fit easily. To verify the influence of the anion binding on the reaction selectivity, we performed control experiments with the neutral acids **1b−8b** and their methyl esters **1c−8c** (Table 1 and Table S2), substrates that do not bind in the DIM pocket of the catalyst (vide supra). As anticipated, the shortest substrate **1a** is hydroformylated with poor selectivity, and hardly any difference in reactivity is observed between this anionic substrate and its acid (**1b**) and ester (**1c**) analogues. The linear/branched selectivity (l/b product ratio) is in the expected range for these substrates, between 1.6 and 2.6. In sharp contrast, substrate **2a**

Table 1. Hydroformylation of Anionic Substrates 1a−8a and Control Experiments[a]

no.	ligand	substrate	n	conversion (%)	regioselectivity (l/b ratio)
1	L1	1a	1	23	2.6
2	L1	2a	2	95 (80)[b]	40 (66)[b]
3	L1	3a	3	85	22
4	L1	4a	4	77	27
5	L1	5a	5	58	19
6	L1	6a	6	56	24
7	L1	7a	7	45	20
8	L1	8a	8	42	15
9	L1	1b	1	46	1.4
10	L1	1c	1	46	1.6
11	L1	2b	2	49	3.7
12	L1	2c	2	42	3.6
13[c]	L1	2c	2	43	3.6
14[d]	L1	2c	2	34	3.9
15[e]	L1	2c	2	27	3.5
16	R1/PPh$_3$	2a	2	100	2.9
17	PPh$_3$	2a	2	100	3.1
18		2a	2	13	1.8

[a]Reagents and conditions: $[Rh(acac)(CO)_2]/L1(R1$ and/or PPh$_3$)/substrate = 1:3(3 and/or 6):100; c(Rh) = 2 mM, 20 bar CO/H$_2$ (1:1), CH$_2$Cl$_2$, 40 °C, 24 h, N,N-diisopropylethylamine (DIPEA, 1.5 equiv) was used as a base for anionic substrate generation; triethylamine (TEA) can be used alternatively. Regioselectivity and conversion (%) were determined by ^{1}H NMR analysis of the reaction mixture. Isomerization and hydrogenation side reactions were not observed. [b]Values between parentheses are for the reaction at room temperature for 72 h. [c]Reaction in the presence of DIPEA (0.3 M). [d]Reaction in the presence of acetic acid (0.2 M). [e]Reaction in the presence of a mixture of acetic acid and DIPEA (0.2 and 0.3 M, respectively). For full experimental details, see the Supporting Information.

(4-pentenoate anion) that precisely spans the distance between the metal and the DIM pocket is hydroformylated with unprecedented selectivity for the linear aldehyde (l/b ratio of 40). If the reaction is carried out at room temperature (instead of 40 °C), the l/b ratio reaches 66. In contrast, the neutral acid (**2b**) and the methyl ester (**2c**) analogues of **2a**, substrates of the same size that do not bind to the DIM binding site of the ligand, form the aldehyde with the typical low selectivity (l/b ratios of ca. 3), verifying the importance of the anion binding. These results demonstrate that for anionic **2a** the reaction barrier for the formation of the linear aldehyde is effectively lowered, with respect to that for the branched product, by the substrate binding event. Interestingly, along with the higher selectivity, the conversion is also much higher when the substrate binds in the DIM pocket of the ligand. The observed rate acceleration can result from the overall lowered reaction barrier due to the substrate preorganization, as well as from the higher concentration of the olefin near the metal center due to substrate prebinding to the DIM pocket of the ligand; that is, the so-called effective concentration[25] of the olefin is substantially higher than the actual concentration of the olefin in solution. Obviously, both effects can contribute simultaneously to the overall increase in rate.

Control experiments confirmed that the presence of acetate ions has negligible effect on the regioselectivity and activity of the Rh(**L1**) catalyst for nonanionic substrates, for example, methyl 4-pentenoate (**2c**) (Table 1, entries 12−15). To further verify that the anion binding site and the catalytic center must

10819

dx.doi.org/10.1021/ja4046235 | J. Am. Chem. Soc. 2013, 135, 10817−10828

be present as an integrated system, we performed a control experiment using a mixture of the anion receptor **R1** (Figure 2) and triphenylphosphine (PPh$_3$). In this case, substrate **2a** (4-pentenoate anion) is hydroformylated with low selectivity, nearly the same as displayed by the catalyst based on only triphenylphospine (Table 1, entries 16 and 17). In the absence of any phosphorus ligand, substrate **2a** is also hydroformylated with poor selectivity (l/b = 1.8) and low conversion (Table 1, entry 18).

Substrates **3a–8a** (5-hexenoate through 10-undecenoate anions) that are the longer homologues of the optimal substrate **2a** also experience an effect of binding in the DIM pocket of the ligand (Table 1). These substrates are hydroformylated with higher selectivity for linear products than their acid **3b–8b** or ester analogues **3c–8c**. In these reactions, the l/b ratios are larger than 15 and therefore all considerably higher than that for the substrates that do not bind to the DIM pocket of the ligand (Table S2). Notably, both the regioselectivity and the rate enhancement (based on conversion) gradually drop with the increasing distance between the anion and the alkene of the substrate (i.e., from **2a** to **8a**). This trend can be explained by the aforementioned effective concentration once the alkene is bound in the DIM pocket of the catalyst, which depends on the inverse cube of the linker length.[25] Consequently, with larger substrates the effective concentration of alkene is lower, hence the reaction is slower, and the alternative pathway via the nonbound species (that is the nonselective "background reaction") contributes effectively, lowering to some extent the overall selectivity of the reaction. Also, the longer substrates lead to complexes with less perturbed alkene coordination, which could affect their reactivity (vide infra). Interestingly, for the longest substrate **8a**, the conversion is similar to that for ester **8c**; however, the selectivity is still enhanced. Notably, among the series of substrates **1a–8a**, the highest regioselectivity and the highest rate enhancement were achieved for substrate **2a**, 4-pentenoate anion that fits precisely in the catalytic cavity, which is between the DIM pocket and the rhodium center.

To further investigate the substrate scope, we also evaluated a small series of (deprotonated) substituted 4-pentenoate acids **9–11** (Scheme 2 and Table 2). These experiments show that

Scheme 2

9 R=CH$_3$, R'=R''=H
10 R=R'=H, R''=CH$_3$
11 R=H, R'=R''=CH$_3$
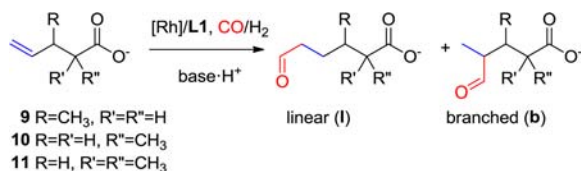
the Rh(**L1**) catalyst stays highly selective as long as the substituents introduced do not hamper the bifunctional substrate binding (Table 2, entries 1,2 vs entry 3).

In view of the high affinity of the DIM binding site for phosphate anions (vide supra), we next extended the scope of substrates to alkenes functionalized with the phosphate group (Scheme 3 and Table 2). One might expect that substrate **13a**, 3-butenylphosphonate anion that is a phosphate analogue of **2a**, would react with similar high selectivity. Indeed, substrate **13a** is hydroformylated by the Rh(**L1**) catalyst to form the linear aldehyde with excellent regioselectivity (l/b > 40). Again, the high selectivity and higher conversion are observed only when

Table 2. Hydroformylation of Substrates 9–13[a]

no.	substrate	n	conversion (%)	regioselectivity (l/b ratio)
1	**9**		79	>100
2	**10**		84	28
3	**11**		22	13
4	**12a**	1	10(69)[b]	– (1.6)[b]
5	**12b**	1	0[c]	
6	**12c**	1	3	0.6
7	**13a**	2	100	>40
8	**13b**	2	0[c]	
9	**13c**	2	12	4.0

[a]Reagents and conditions: [Rh(acac)(CO)$_2$]/**L1**/substrate = 1:3:100; c(Rh) = 2 mM, 20 bar CO/H$_2$ (1:1), CH$_2$Cl$_2$, 40 °C for entries 1–3 and room temperature for entries 4–9, 24 h, N,N-diisopropylethyl-amine (DIPEA, 1.5 equiv for **9–11** and 3 equiv for **12a** and **13a**) was used as a base for anionic substrate generation. Regioselectivity and conversion (%) were determined by ^{1}H and/or ^{13}C NMR analysis of the reaction mixture. Isomerization and hydrogenation side reactions were not observed. [b]At room temperature, the conversion is too low to determine the selectivity; values between parentheses are for the reaction at 40 °C. [c]Additional experiments with 1-octene showed that under these strongly acidic conditions the catalyst is inactive. For full experimental details, see the Supporting Information.

Scheme 3
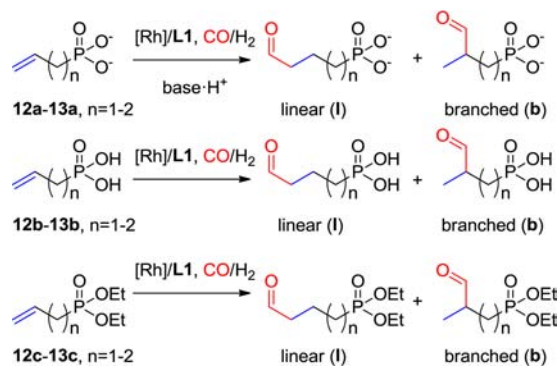
the anionic substrate is used (Table 2, entries 7–9). As expected, the homologue **12a**, allyl-phosponate anion that is too short to span the distance between the catalytic and the binding site, is converted with low regioselectivity (Table 2, entries 4 and 6).
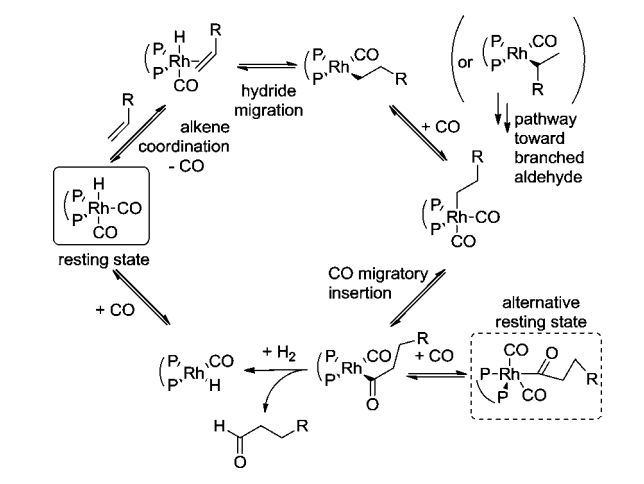
Kinetic Studies and Mode of Action. To gain a deeper insight into the reaction mechanism, we studied the hydroformylation of substrate **2a** by Rh(**L1**) in more detail. In situ HP IR spectroscopy identifies the hydrido complex [Rh(**L1**)-(CO)$_2$H] as the resting state of the catalyst throughout the whole catalytic experiment.[24] Monitoring reaction progress by the gas-uptake for experiments with different partial pressures of CO and H$_2$ reveals the (nearly) zero-order dependence of the reaction rate (turnover frequency, TOF, consumed substrate/catalyst/time in mol mol^{-1} h^{-1}) on the hydrogen pressure and the negative dependence of the TOF on the pressure of CO (Table 3). Furthermore, experiments with different substrate concentrations reveal the positive dependency of the TOF on the alkene concentration (Table 3). Thus, both in situ HP IR spectroscopy and gas-uptake experiments are in agreement with a rate-determining step early in the catalytic cycle (Scheme 4), being either alkene coordination or hydride migration.[3]

Table 3. Hydroformylation of Substrate 2a by Rh(L1)^a

no.	$c(2a)$ (M)	$P(H_2)$ (bar)	$P(CO)$ (bar)	TOF
1	1.0	10	10	24
2	1.0	10	20	11
3	1.0	20	10	25
4	1.0	20	20	13
5	0.5	10	10	19
6	0.2	10	10	15
7	0.1	10	10	13

^{a}Reagents and conditions: $[Rh(acac)(CO)_2]/L1$ = 1:1.5; $c(Rh)$ = 2 mM, CH_2Cl_2, 40 °C, triethylamine (TEA, 1.5 equiv) was used as a base for anionic substrate generation. Turnover frequency, TOF (mol mol^{-1} h^{-1}), was determined from gas-uptake profiles at 10% conversion. For full experimental details, see the Supporting Information.

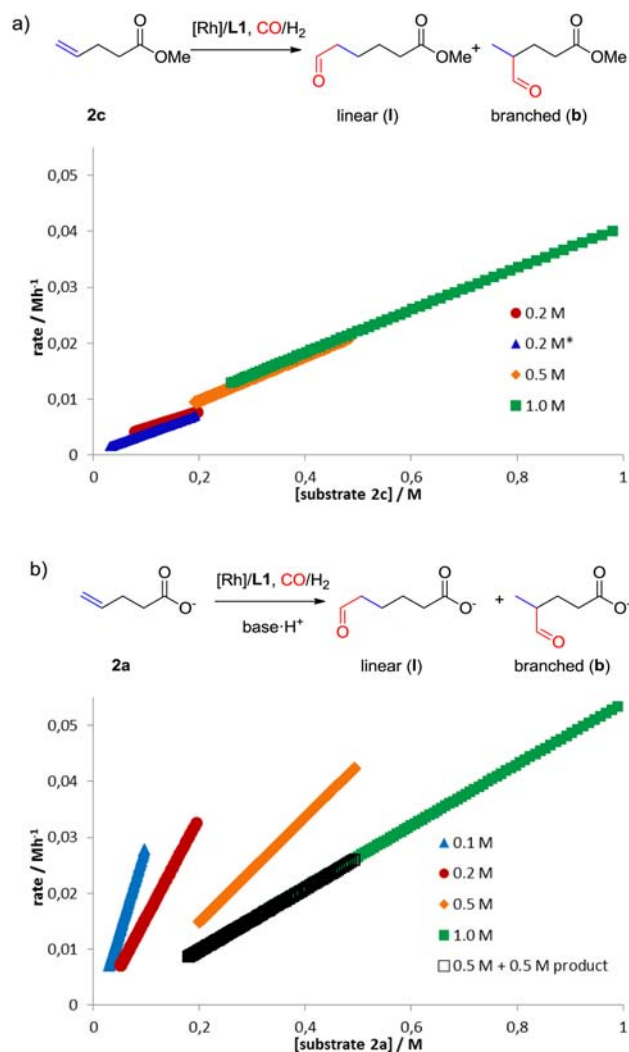**Scheme 4. Catalytic Cycle of the Rhodium-Catalyzed Hydroformylation**

Figure 3. Graphical representation of the kinetic profiles: reaction rate versus substrate concentration plots from reaction at different initial substrate concentrations for hydroformylation of ester **2c** (a) and anionic **2a** (b) using Rh(**L1**) as the catalyst, determined by gas uptake methods. Reagents and conditions: 20 bar CO/H$_2$ (1:1), CH$_2$Cl$_2$, 40 °C, $[Rh(acac)(CO)_2]/L1$ = 1:1.5; $c(Rh)$ = 2 mM, triethylamine (TEA, 1.5 equiv) was used as a base for anionic substrate generation, and pentanoic acid was used to mimic the product (the aldehyde group is proven not to affect the kinetics) (* = repeated experiment with a longer reaction time). For full experimental details, see the Supporting Information.

Reaction progress kinetic analysis[26] for experiments under the standard conditions (CO/H$_2$ 1:1, 20 bar (constant pressure), 40 °C) provides further insight into the reaction mechanism. The initial studies were performed for ester **2c** (methyl 4-pentenoate), that is, the substrate, which does not bind in the DIM pocket of the Rh(**L1**) catalyst. These experiments reveal, common for hydroformylation,[3b] the first-order dependence of the reaction rate on the substrate concentration (the first-order constant, k_1 = 0.0458 h^{-1}; eq 1). Furthermore, no catalyst inhibition by the product was observed, as indicated by the overlying curves, in Figure 3a.[26]

$$V = k_1 \cdot [S] \tag{1}$$

Additionally, this analysis shows that the catalyst activation period is negligible and that there is no catalyst deactivation occurring during the reaction triggered by the substrate or the product. Both of these findings stay in agreement with the in situ HP IR and HP NMR studies, which showed the fast catalyst activation (<15 min at 40 °C) and no catalyst decomposition within at least 48 h.

In contrast, the reaction progress kinetic analysis for the hydroformylation of anionic alkene **2a** (4-pentenoate), which is the substrate that does bind in the binding site of the Rh(**L1**) catalyst, demonstrates a different kinetic behavior (under otherwise identical conditions, Figure 3b). Experiments at different initial substrate concentrations (0.1−1.0 M of **2a**) reveal a linear dependence of rate on substrate concentration

for an individual experiment; yet the reaction kinetics is also strongly dependent on the initial substrate concentration (nonoverlying blue, red, orange, and green curves, Figure 3b). This observation could indicate either slow catalyst deactivation during the course of the reaction or catalyst inhibition by the product formed.[26] To discriminate between these scenarios, we performed an additional experiment using a mixture of 0.5 M of the substrate and 0.5 M of the product, simulating the reaction performed with the initial substrate concentration of 1 M being halfway executed. As is clear from Figure 3b, the reaction rate versus substrate concentration plots from these experiments overlay perfectly (green and black curves, Figure 3b), in contrast to that for the experiment with the initial substrate concentration of 0.5 M (orange curve, Figure 3b). These experiments indicate that the catalyst is

stable and that the reaction is inhibited to some extent by the product that is formed. Such behavior is in line with a mechanism in which the substrate is preorganized in the binding site of the catalyst prior to reacting on the metal center. Such system should follow Michaelis−Menten kinetics with a competitive product inhibition (eq 2; V = reaction rate (in M h^{-1}), V_{max} = maximum reaction rate (in M h^{-1}), K_{mm} = Michaelis constant (in M), K_i = product inhibition constant (in M), [S] = substrate concentration (in M), and [P] = product concentration (in M)).[27]

$$V = \frac{V_{max} \cdot [S]}{K_{mm} + [S] + \frac{K_{mm}}{K_i} \cdot [P]} \tag{2}$$

Indeed, the reaction progress data gave a good fit to eq 2, revealing the following kinetic parameters: V_{max} = 0.063 M h^{-1}, K_{mm} = 0.168(5) M, and K_i = 0.158(4) M. Nearly equal values of the Michaelis constant and the product inhibition constant show that both the substrate and the product interact with the catalyst in a similar fashion. This indicates that they compete for the binding in the DIM pocket (rather than for the metal center). Thus, the product inhibits the reaction via partial expelling of the substrate from the DIM pocket, hence lowering its "local concentration". In view of the nearly equal values of K_{mm} and K_i, and the stoichiometry of the reaction (one molecule of the product formed for one molecule of the substrate reacted, hence the sum of [S] and [P] being equal to the initial substrate concentration (c_0)), eq 2 can be simplified:

$$K_{mm} \cong K_i$$

and

$$[S] + [P] = c_0$$

Thus, in this case, eq 2 simplifies to:

$$V = \frac{V_{max} \cdot [S]}{K_{mm} + c_0} \tag{3}$$

Equation 3 shows and rationalizes the pseudo-first-order dependence of the reaction rate on the substrate concentration observed experimentally for individual experiments (Figure 3b) and shows the influence of the initial substrate concentration on the reaction kinetics.

The evaluation of the influence of the concentration of substrate **2a** on its hydroformylation reveals that the selectivity gradually drops with higher initial concentrations; however, it does not change during the single experiment (the l/b ratio = 52, 44, 22, and 15 at 0.1, 0.2, 0.5, and 1.0 M solution of **2a**, respectively, and the l/b = 15 at 0.5 M solution of **2a** in the presence of 0.5 M of the product). This shows that at higher concentrations a greater part of the reaction occurs along a nonselective pathway with more substrate and product molecules involved. Higher concentrations favor a scenario in which the anionic functionality of the reactive substrate is not bound in the DIM binding site, because the latter is already occupied by another molecule (substrate or product formed). Thus, this transformation does not experience any substrate preorganization and leads to a mixture of both products (in analogy to reaction with nonanionic substrates). This stays in agreement with DFT calculations, which suggest that the branched aldehyde cannot be formed when its anionic moiety is bound in the DIM binding site of the catalyst (vide infra).

To investigate the relative substrate selectivity, we next performed competition experiments with mixtures of substrates. Competitive hydroformylation of substrate **2a** that precisely fits to the Rh(**L1**) system, and of its methyl ester analogue (**2c**), shows that at first mostly anionic substrate is consumed, while during that reaction period ester **2c** reacts slowly (Figure 4a). During the course of the reaction, when a
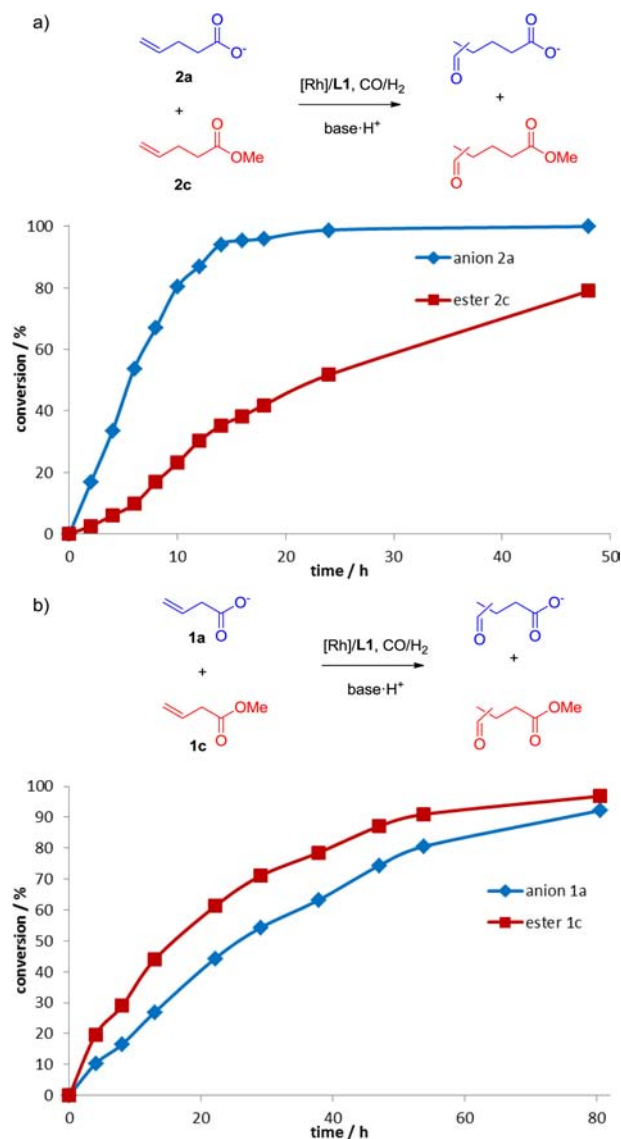

Figure 4. Substrate competition experiments: hydroformylation of a 1:1 mixture of substrates **2a** and **2c** (a) and **1a** and **1c** (b) by Rh(**L1**). Reagents and conditions: 20 bar CO/H$_2$ (1:1), CH$_2$Cl$_2$, 40 °C, [Rh(acac)(CO)$_2$]/**L1**/substrate I/substrate II = 1:3:100:100; c(Rh) = 2 mM, N,N-diisopropylethylamine (DIPEA, 1.5 equiv) was used as a base for anionic substrate generation. For full experimental details, see the Supporting Information.

greater part of **2a** is consumed (and the anionic product formed competes for the binding to the DIM binding site with remaining substrate **2a** (vide supra)), ester substrate **2c** is converted more quickly (Figure 4a). Kinetic analysis shows that anion **2a** reacts with the overall first-order kinetics (Figure S20), despite the competition with ester **2c**, as in the single substrate experiments (vide supra). Interestingly, ester **2c** reacts at first with the seeming negative order kinetics that during the

course of the reaction (conversion of **2a** > 60%) switches to the expected first-order kinetics (Figure S20). This indicates that initially the preassociation of **2a** with the DIM pocket of Rh(**L1**) increases its "effective concentration" around the catalytic metal center, outcompeting substrate **2c**, but in the final phase of the reaction this effect is attenuated due to product inhibition (vide supra).

In contrast, the competition experiment with the shortest substrate **1a**, which is too short for bifunctional binding to Rh(**L1**), and with its methyl ester **1c**, shows that both substrates react rather independently of each other (Figure 4b), and both follow first-order kinetics (Figure S21). Interestingly, in this case, ester **1c** reacts a bit faster than anionic **1a**. Presumably, the latter being bound in the anion binding site needs to dissociate prior to reacting on the metal center, resulting in its lower reactivity. Furthermore, the competition experiment between anionic substrates **1a** and **2a** shows similar reactivity trends (Figure 5) with the first-order kinetics (Figure
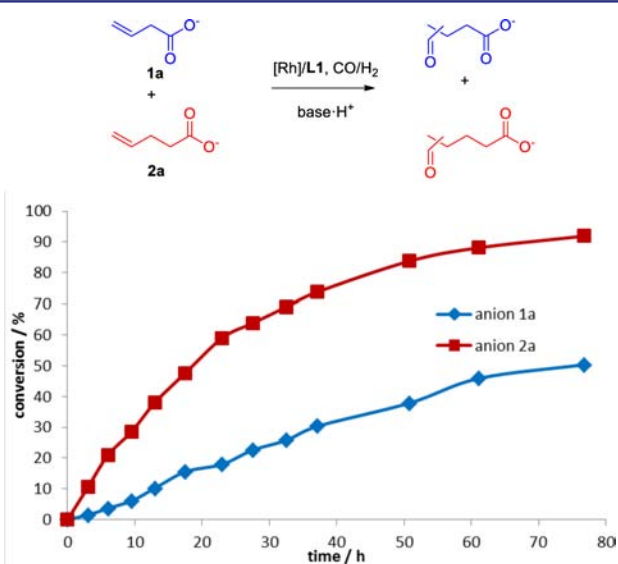

Figure 5. Competitive hydroformylation of a 1:1 mixture of substrates **1a** and **2a** by Rh(**L1**). Reagents and conditions: 20 bar CO/H$_2$ (1:1), CH$_2$Cl$_2$, 40 °C, [Rh(acac)(CO)$_2$]/**L1**/**1a**/**2a** = 1:3:100:100; c(Rh) = 2 mM, triethylamine (TEA, 1.5 equiv) was used as a base for anionic substrate generation. For full experimental details, see the Supporting Information.

S22), demonstrating that both compete for the binding site equally. However, substrate **2a** reacts faster, because it can react more easily on the metal center when its anionic group is bound in the DIM pocket, while substrate **1a** needs to dissociate from the DIM binding site prior to reacting on the metal center, lowering its reactivity. Additionally, the competition experiment between the longest anionic substrate **8a** and ester **1c** shows that both substrates seem to react independently of one another, both following first-order kinetics (Figure S23). This reveals that, at the concentrations used, the effective concentration of the long substrate **8a** is comparable to the actual concentration in solution.[28] Therefore, the substrate prebinding does not lead to the effective competition with the nonbinding substrate **1c**, and hence does not inhibit the intermolecular hydroformylation. This confirms that the effective concentration that depends inversely on the cube of the linker length[25] is of crucial importance in determining the (relative) reaction rate, which is found both

in the competition experiment, as well as in the rate enhancement for shorter substrate **2a** as compared to **8a**.

Taking all of these results together, these experiments reveal the order of the events taking place on the catalyst. First, the substrate molecule is bound via the anionic group to the binding site of the catalyst (rather than the double bond coordinates first). Next, if the CO dissociates from the rhodium center, the double bond can coordinate to it and follow the catalytic cycle (Scheme 4), which is finished by the product release. The equilibrium between the free substrate and that bound in the DIM pocket is fast compared to the alkene conversion.

DFT Calculations and Origin of Selectivity. To gain deeper understanding of the origin of the selectivity, we studied the Rh(**L1**) catalytic system with DFT (BP86, SV(P)). Both in situ IR and kinetic studies (vide supra) show that the rate-determining step is early in the catalytic cycle, which in combination with the absence of double bond isomerization indicates that the regioselectivity for this catalytic system is defined during insertion of the olefin into the Rh−H bond. We additionally confirmed this by performing experiments using D$_2$/CO. Under these conditions, deuterium scrambling was not observed (Figure S24), which indicates that the hydride migration step is indeed irreversible.[24,29] Consequently, this selectivity determining hydride migration step was further studied in detail.

We first calculated several possible structures of the substrate−catalyst complex [RhH(CO)(**L1**)]−(**2a**) with different geometries around the metal center.[30] We found that the eq−eq coordination geometry is preferred over the eq−ax isomeric complex by 17.7 kJ/mol (**I** and **V** in Figure 6). The optimal eq−eq complex structure shows that the carboxylate group of the substrate is strongly bound in the DIM pocket of the ligand with four hydrogen bonds ($d_{N−O}$ = 2.7−2.9 Å), and the coordinated alkene moiety is tilted out of the P−Rh−P plane of the trigonal bipyramidal rhodium complex (**I** in Figure 6). This perturbation results from the carboxylate moiety being anchored in the binding site of the ligand. Importantly, the anionic group binding severely restricts the movement of the coordinated double bond. However, the double bond can easily rotate toward the transition state, leading to the linear alkyl Rh complex, and hence to the linear aldehyde product. In fact, the geometry of the complex in the calculated early transition state ($\Delta G^{\circ\ddagger}$ = 11.2 kJ mol^{-1}) is almost unperturbed (the Rh−H bond elongates by only 0.036 Å), with the alkene rotated only a little further out of the equatorial plane (**II** in Figure 6). Restrictions on the movement of the double bond imposed by the bifunctional substrate binding block its rotation in the direction necessary for the reaction pathway toward the branched alkyl Rh;[31] hence the branched aldehyde product cannot be formed from this complex conformer. The alternative conformer of the substrate−catalyst complex in which the carbonyl and hydride positions are inverted (**IV** in Figure 6), hence for which the favored rotation of the alkene would direct the reaction toward the branched product, was also evaluated. This conformation has a much higher energy (15.8 kJ mol^{-1})[32] that is even higher than the transition state leading to the linear product from the former substrate−catalyst conformer ($\Delta\Delta G^{\circ}$ = 4.6 kJ mol^{-1}). These calculations suggest that the branched aldehyde product that is formed during the reaction follows a pathway in which the anion moiety of the substrate is not bound in the DIM pocket of the ligand (e.g.,
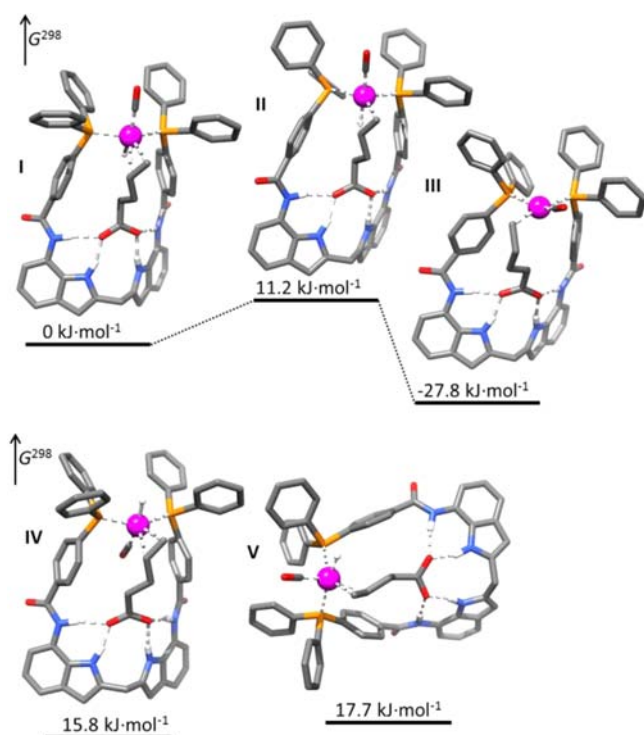
Figure 6. Calculated reaction pathway (DFT, BP86, SV(P)) of the regioselectivity-determining hydride migration step in the hydroformylation of substrate **2a** by the Rh(**L1**) catalyst. Notation: catalyst–substrate complex **I**, transition state toward linear product **II**, and linear alkyl Rh complex **III**, alternative structures of the catalyst–substrate complex **IV** and **V**. G^{298}: Gibbs free energy at 298 K (relative to the catalyst-substrate complex **I**) in kJ mol^{-1}. For full computational details, see the Supporting Information.

Figure 7. Calculated reaction pathway (DFT, BP86, SV(P)) of the regioselectivity-determining hydride migration step in the hydroformylation of substrate **3a** (a) and **4a** (b) by the Rh(**L1**) catalyst. Notation: catalyst–substrate complex **I**, transition state toward linear product **II**, and linear alkyl Rh complex **III**. G^{298}: Gibbs free energy at 298 K (relative to the catalyst–substrate complex **I**) in kJ mol^{-1}. For full computational details, see the Supporting Information.

the anion binding site is occupied by another substrate molecule or by the product formed, vide supra).

Calculations for reactions with longer substrates **3a** and **4a** reveal similar trends for the hydride migration step (Figure 7). The main difference is that the longer aliphatic linkers between the double bond and the carboxylic moiety allow one to more easily span the distance between the metal center and the anion binding site, resulting in less perturbed coordination of the alkene moiety in the equatorial plane of the Rh(**L1**) complex. Thus, the double bond needs to rotate slightly further to reach the transition state leading to the linear product. However, this is still the privileged direction of the alkene rotation, due to the restrictions imposed by the substrate anchoring in the DIM pocket. Moreover, the lower perturbation of the alkene coordination for longer substrates results in the greater difference between the substrate–catalyst complex and the decisive transition state. This in turn results in a higher energy barrier. This, together with the change in the effective concentration, explains why the longer anionic substrates have a lower rate enhancement with respect to their ester analogues in comparison to the substrate **2a** that fits best (vide supra).

These DFT studies corroborate our assertion that the high regioselectivity obtained for size-matching substrates with the Rh(**L1**) catalyst originates from substrate preorientation imposed by the hydrogen bonds between the anionic functionality and the DIM pocket. This interaction highly restricts the movement of the reactive double bond during the decisive selectivity-determining step. Preorganization favors the
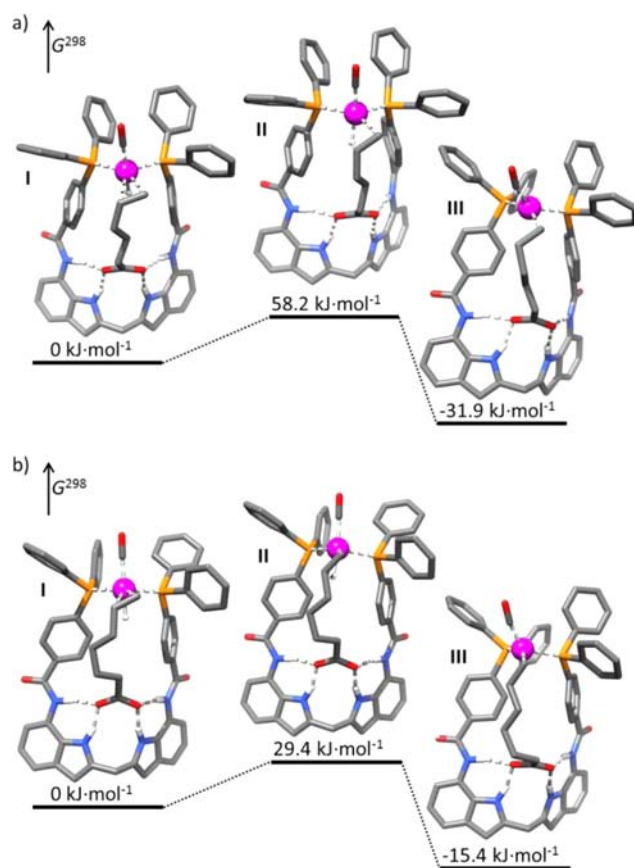
reaction pathway that leads to the linear aldehyde and hinders the competing pathway that would lead to the isomeric product.

Regioselective Hydroformylation of Internally Unsaturated Aliphatic Acids. Selective hydroformylation of internal alkenes is highly challenging, as it involves an internal double bond with inherent lower reactivity. More forcing conditions in turn lead to possible isomerization side reactions,[2] which are deteriorating the selectivity.[33] Moreover, to be selective, the catalyst needs to precisely differentiate between carbon atoms of the double bond whose electronic properties are nearly identical. Importantly, analysis of the mechanism controlling the regioselectivity for hydroformylation of terminal olefins **1a**–**8a** with the Rh(**L1**) catalyst (Figures 6 and 7) allows one to postulate that the approach should be also operative for substrates with internal double bonds. In principle, one may expect that the restricted movement of the reactive functionality should allow for selective introduction of the aldehyde moiety on the carbon atom of the double bond, which is more distant from the carboxylic group. Unfortunately, our initial hydroformylation experiments proved that the Rh(**L1**) catalyst is not active enough for substrates with internal double bonds. Therefore, we next investigated the optimization of the activity for this catalytic system by modifying the DIMPhos ligand.

Less basic phosphine and more π-accepting phosphite ligands are known to afford more active rhodium complexes for hydroformylation.[34,35] We therefore designed and prepared ligand **L2**, a close analogue of **L1** functionalized with two strongly electron-withdrawing trifluoromethyl groups on each of the four phenyl rings (Figure 2). We also obtained ligand **L3**, equipped with phosphite donor atoms (Figure 2), which are known to lead to highly reactive hydroformylation catalysts.[35a]

To evaluate the influence of the modifications introduced, ligands **L2** and **L3** were first studied in the hydroformylation of anionic terminal olefins **1a–8a** (under otherwise identical conditions). In general, ligands **L1–L3** allow for hydroformylation of all substrates **1a–8a** with remarkable regioselectivities, with the l/b ratios all above 38. The trends of relative selectivity are somewhat different (Figure 8), and they cannot
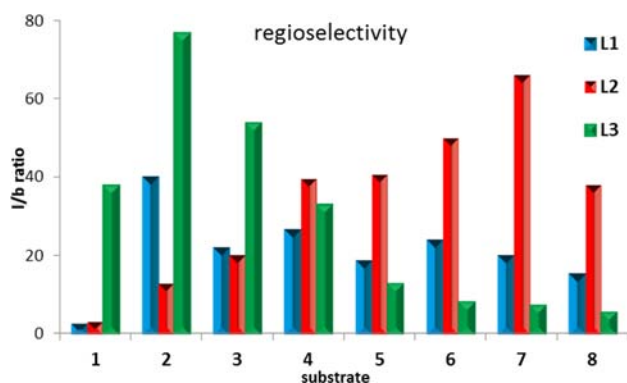

Figure 8. Hydroformylation of anionic substrates **1a–8a** using Rh– ligands **L1–L3** catalysts. Full conversion in all cases for catalysts with ligands **L2,L3**; for conversion with ligand **L1**, see Table 1. Conditions are as described in the footnote to Table 1, with **L2**/Rh = **L3**/Rh = 1.1. For full experimental details, see the Supporting Information.

be fully rationalized at this point. Interestingly, when phosphite ligand **L3** was applied, also the shortest substrate **1a** reacts with very high selectivity (l/b = 38), in contrast to results for catalysts with phosphine ligands **L1**, **L2**. To rationalize this, we performed DFT studies for the Rh(**L3**)–(**1a**) complex. The molecular modeling shows that the higher flexibility of this phosphite-based ligand allows one to reduce the distance between the metal center and the anion binding site such that the Rh(**L3**) can adjust for bifunctional binding to substrate **1a** (Figure 9). Again, the double bond can rotate more easily in one direction, leading to regioselective hydroformylation of the bound substrate (Figures S22). The activities displayed by catalysts with all DIMPhos ligands **L1–L3** were further compared quantitatively in hydroformylation of model
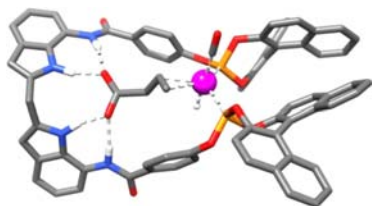

Figure 9. Calculated structure (DFT, BP86, SV(P)) of the catalyst– substrate complex [RhH(CO)(**L3**)]–(**1a**). For reaction pathways of the regioselectivity-determining hydride migration step in the hydroformylation of substrate **1a** by the Rh(**L3**) catalyst, see Figure S26.

substrate **2a**, revealing TOFs of 24, 86, and 100 mol mol^{-1} h^{-1}, for **L1**, **L2**, and **L3**, respectively, proving the successful design of new ligands.

With more active catalysts in hand, we evaluated the hydroformylation of aliphatic carboxylates with internal double bonds. Although more reactive than Rh(**L1**), the catalyst with phosphine ligand **L2** did not afford sufficient activity to convert internal alkenes. Fortunately, the catalyst based on phosphite **L3** proved to be active toward these substrates, providing close to full conversion for most of the reactions (Scheme 5 and

Scheme 5

14 n=1, R=(E)-CH$_3$
15 n=1, R=(E)-C$_2$H$_5$
16 n=1, R=(E/Z)-C$_3$H$_7$
17 n=1, R=(E/Z)-C$_4$H$_9$
18 n=2, R=(E/Z)-CH$_3$
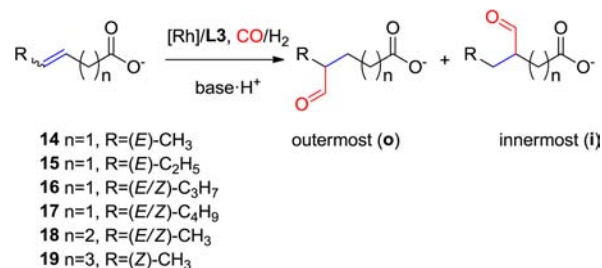**19** n=3, R=(Z)-CH$_3$

Table 4). Interestingly, the catalyst is highly precise, presenting unprecedented regioselectivities for the whole range of substrates that differ in the positions of the reactive double bond with respect to the carboxylic functionality and in size of the substituents (Table 4). In addition, both E and Z isomers of the substrates are converted with high selectivity. The analysis of the isolated products shows that, as anticipated, in all cases

Table 4. Hydroformylation of Internal Alkenes 14–19[a]

no.	substrate	major product	conv. (%)	regioselect. (o/i ratio)
1	14		94	23
2	15		95	25
3	16		86	27
4	17		82	26
5	18		>99	78
6	19		95	27

[a]Reagents and conditions: [Rh(acac)(CO)$_2$]/**L3**/substrate = 1:1.1:100; [Rh] = 2 mM, 20 bar CO/H$_2$ (1:1), CH$_2$Cl$_2$, 40 °C, 72 h, triethylamine (TEA, 1.5 equiv) was used as a base for anionic substrate generation. Regioselectivity and conversion (%) were determined by ^{1}H NMR analysis of the reaction mixture. For full experimental details, see the Supporting Information.

the major product has the aldehyde functionality on the carbon atom of the double bond more distant from the carboxylate group (Table 4). The relative selectivity of addition of the aldehyde group across the double bond is above 23 in all cases; hence the major product is formed with regioselectivity above 95%![36] For comparison, typical catalysts provide close to equimolar mixtures of alternative products. For example, for Rh−PPh$_3$ catalyst, the ratio between products is in the range 0.8 and 1.7 (under otherwise identical conditions).[24] Importantly, for reactions with Rh(**L3**) at higher temperatures, the regioselectivity is retained at a similar level, allowing for greater catalyst activity, however, at the expense of some side/consecutive reactions.[24] These results further confirm the general operational model of the Rh−DIMPhos catalysts.

CONCLUSION

In summary, we have reported a series of DIMPhos ligands **L1**−**L3**, which are bidentate phosphorus ligands equipped with an integral anion binding site (the DIM pocket). We have shown that these bifunctional ligands form well-defined rhodium complexes that can bind anionic species in the binding site of the ligand. This interaction can be used to preorganize a substrate molecule, that is, an alkene with an anionic group that can be remote from the reactive double bond (even 10 bonds!), which leads to its highly selective hydroformylation. For the hydroformylation of substrates with internal double bonds, the current system gives the highest selectivity reported in the literature,[37] clearly demonstrating the power of supramolecular control of the selectivity for catalysis. Importantly, the mode of operation is well understood by the detailed studies provided in this Article. This enables rational design of selective catalysts for desired reactions, clearly complementing trial-and-error approaches in the field of transition metal catalysis. In principle, it should be possible to transmit the current system to other transition metal-catalyzed processes involving a migration in the selectivity-determining step, giving rise to other selective transformations in chemical catalysis. Research along these lines is continued in our laboratories.

ASSOCIATED CONTENT

S Supporting Information

Details concerning materials and methods, catalytic and kinetic studies, coordination and binding studies, DFT studies, experimental procedures, and spectral data for new compounds (including images of NMR spectra). This material is available free of charge via the Internet at http://pubs.acs.org.

AUTHOR INFORMATION

Corresponding Author
j.n.h.reek@uva.nl
Notes
The authors declare no competing financial interest.

ACKNOWLEDGMENTS

REFERENCES

(1) Beller, M. *Chem. Soc. Rev.* **2011**, *40*, 4891−4892.

(2) (a) Cornils, B., Herrmann, W. A., Eds. *Applied Homogeneous Catalysis with Organometallic Compounds: A Comprehensive Handbook in Three Volumes*, 2nd ed.; Wiley-VCH: Weinheim, 2002. (b) Beller, M., Bolm, C., Eds. *Transition Metals for Organic Synthesis*; Wiley-VCH: Weinheim, 2004.

(3) (a) Hartwig, J. F. *Organotransition Metal Chemistry: From Bonding to Catalysis*; University Science Books: Sausalito, 2009. (b) van Leeuwen, P.W. N. M. *Homogeneous Catalysis: Understanding the Art*; Kluwer Academic Publishers: Dordrecht, 2004.

(4) For reviews, see: (a) Goudriaan, E. P.; van Leeuwen, P.W. N. M.; Birkholz, M.-N.; Reek, J. N. H. *Eur. J. Inorg. Chem.* **2008**, 2939−2958. (b) Breit, B. *Pure Appl. Chem.* **2008**, *80*, 855−860. (c) Reetz, M. T. *Angew. Chem., Int. Ed.* **2008**, *47*, 2556−2588. (d) de Vries, J. G.; de Vries, A. H. M. *Eur. J. Org. Chem.* **2003**, 799−811. (e) Gennari, C.; Piarulli, U. *Chem. Rev.* **2003**, *103*, 3071−3100. (f) Tang, W.; Zhang, X. *Chem. Rev.* **2003**, *103*, 3029−3070. (g) Jäkel, C.; Paciello, R. *Chem. Rev.* **2006**, *106*, 2912−2942. For supramolecular ligand strategies, see: (h) Wilkinson, M. J.; van Leeuwen, P. W. N. M.; Reek, J. N. H. *Org. Biomol. Chem.* **2005**, *3*, 2371−2383. (i) Breit, B. *Angew. Chem., Int. Ed.* **2005**, *44*, 6816−6825. (j) Sandee, A. J.; Reek, J. N. H. *Dalton Trans.* **2006**, 3385−3391. (k) Meeuwissen, J.; Reek, J. N. H. *Nat. Chem.* **2010**, *2*, 615−621.

(5) (a) Whisler, M. C.; MacNeil, S.; Snieckus, V.; Beak, P. *Angew. Chem., Int. Ed.* **2004**, *43*, 2206−2225. (b) Snieckus, V. *Chem. Rev.* **1990**, *90*, 879−933. (c) Reetz, M. T. *Acc. Chem. Res.* **1993**, *26*, 462−468. (d) Engle, K. M.; Mei, T.-S.; Wasa, M.; Yu, J.-Q. *Acc. Chem. Res.* **2012**, *45*, 788−802. (e) Colby, D. A.; Tsai, A. S.; Bergman, R. G.; Ellman, J. A. *Acc. Chem. Res.* **2012**, *45*, 814−825. (f) Daugulis, O.; Do, H.-Q.; Shabashov, D. *Acc. Chem. Res.* **2009**, *42*, 1074−1086. (g) Chen, X.; Engle, K. M.; Wang, D.-H.; Yu, J.-Q. *Angew. Chem., Int. Ed.* **2009**, *48*, 5094−5115.

(6) (a) Carboni, S.; Gennari, C.; Pignataro, L.; Piarulli, U. *Dalton Trans.* **2011**, *40*, 4355−4373. (b) Dong, Z.; Luo, Q.; Liu, J. *Chem. Soc. Rev.* **2012**, *41*, 7890−7908. (c) van Leeuwen, P. W. N. M. *Supramolecular Catalysis*; Wiley-VCH: Weinheim, 2008. (d) Crabtree, R. H. *New J. Chem.* **2011**, *35*, 18−23.

(7) (a) Yang, J.; Gabriele, B.; Belvedere, S.; Huang, Y.; Breslow, R. *J. Org. Chem.* **2002**, *67*, 5057−5067. (b) Yang, J.; Breslow, R. *Angew. Chem., Int. Ed.* **2000**, *39*, 2692−2694. (c) Breslow, R.; Zhang, X.; Huang, Y. *J. Am. Chem. Soc.* **1997**, *119*, 4535−4536. (d) Breslow, R.; Zhang, X.; Xu, R.; Maletic, M.; Merger, R. *J. Am. Chem. Soc.* **1996**, *118*, 11678−11679. (e) Fang, Z.; Breslow, R. *Org. Lett.* **2006**, *8*, 251−254. (f) Breslow, R.; Brown, A. B.; McCullough, R. D.; White, P. W. *J. Am. Chem. Soc.* **1989**, *111*, 4517−4518.

(8) For reviews, see: (a) Taylor, M. S.; Jacobsen, E. N. *Angew. Chem., Int. Ed.* **2006**, *45*, 1520−1543. (b) Sohtome, Y.; Nagasawa, K. *Chem. Commun.* **2012**, *48*, 7777−7789. For selected examples, see: (c) Zuend, S. J.; Coughlin, M. P.; Lalonde, M. P.; Jacobsen, E. N. *Nature* **2009**, *461*, 968−970. (d) Xu, H.; Zuend, S. J.; Woll, M. G.; Tao, Y.; Jacobsen, E. N. *Science* **2010**, *327*, 986−990. (e) Singh, R. P.; Foxman, B. M.; Deng, L. *J. Am. Chem. Soc.* **2010**, *132*, 9558−9560. (f) Klauber, E. G.; De, C. K.; Shah, T. K.; Seidel, D. *J. Am. Chem. Soc.* **2010**, *132*, 13624−13626. (g) Wang, Y.; Yu, T.-Y.; Zhang, H.-B.; Luo, Y.-C.; Xu, P.-F. *Angew. Chem., Int. Ed.* **2012**, *51*, 12339−12342. (h) Lu, Y.; Johnstone, T. C.; Arndtsen, B. A. *J. Am. Chem. Soc.* **2009**, *131*, 11284−11285. (i) Bauer, A.; Westkämper, F.; Grimme, S.; Bach, T. *Nature* **2005**, *436*, 1139−1140. (j) Müller, C.; Bauer, A.; Bach, T. *Angew. Chem., Int. Ed.* **2009**, *48*, 6640−6642. (k) Müller, C.; Maturi, M. M.; Bauer, A.; Cuquerella, M. C.; Miranda, M. A.; Bach, T. *J. Am. Chem. Soc.* **2011**, *133*, 16689−16697. (l) Wiegand, C.; Herdtweck, E.; Bach, T. *Chem. Commun.* **2012**, *48*, 10195−10197.

(9) (a) Grotjahn, D. B.; Miranda-Soto, V.; Kragulj, E. J.; Lev, D. A.; Erdogan, G.; Zeng, X.; Cooksy, A. L. *J. Am. Chem. Soc.* **2008**, *130*, 20−21. (b) Grotjahn, D. B.; Kragulj, E. J.; Zeinalipour-Yazdi, C. D.; Miranda-Soto, V.; Lev, D. A.; Cooksy, A. L. *J. Am. Chem. Soc.* **2008**, *130*, 10860−10861.

(10) (a) Das, S.; Incarvito, C. D.; Crabtree, R. H.; Brudvig, G. W. *Science* **2006**, *312*, 1941−1943. (b) Das, S.; Brudvig, G. W.; Crabtree, R. H. *J. Am. Chem. Soc.* **2008**, *130*, 1628−1637. (c) Hull, J. F.; Sauer, E.

L. O.; Incarvito, C. D.; Faller, J. W.; Brudvig, G. W.; Crabtree, R. H. *Inorg. Chem.* **2009**, *48*, 488−495.

(11) (a) Smejkal, T.; Gribkov, D.; Geier, J.; Keller, M.; Breit, B. *Chem.-Eur. J.* **2010**, *16*, 2470−2478. (b) Smejkal, T.; Breit, B. *Angew. Chem., Int. Ed.* **2008**, *47*, 311−315.

(12) (a) Fackler, P.; Berthold, C.; Voss, F.; Bach, T. *J. Am. Chem. Soc.* **2010**, *132*, 15911−15913. (b) Fackler, P.; Huber, S. M.; Bach, T. *J. Am. Chem. Soc.* **2012**, *134*, 12869−12878.

(13) (a) Dzik, W. I.; Xu, X.; Zhang, X. P.; Reek, J. N. H.; de Bruin, B. *J. Am. Chem. Soc.* **2010**, *132*, 10891−10902. (b) Zhu, S.; Ruppel, J. V.; Lu, H.; Wojtas, L.; Zhang, X. P. *J. Am. Chem. Soc.* **2008**, *130*, 5042−5043.

(14) (a) Breuil, P.-A. R.; Patureau, F. W.; Reek, J. N. H. *Angew. Chem., Int. Ed.* **2009**, *48*, 2162−2165. (b) Breuil, P.-A. R.; Reek, J. N. H. *Eur. J. Org. Chem.* **2009**, 6225−6230. (c) Dydio, P.; Rubay, C.; Gadzikwa, T.; Lutz, M.; Reek, J. N. H. *J. Am. Chem. Soc.* **2011**, *133*, 17176−17179.

(15) Sessler, J. L.; Gale, P. A.; Cho, W.-S. *Anion Receptor Chemistry*; Royal Society of Chemistry: Cambridge, 2006. (b) Dydio, P.; Lichosyt, D.; Jurczak, J. *Chem. Soc. Rev.* **2011**, *40*, 2971−2985. (c) Wenzel, M.; Hiscock, J. R.; Gale, P. A. *Chem. Soc. Rev.* **2012**, *41*, 480−520.

(16) (a) Dydio, P.; Zieliński, T.; Jurczak, J. *Chem. Commun.* **2009**, *45*, 4560−4562. (b) Dydio, P.; Zieliński, T.; Jurczak, J. *Org. Lett.* **2010**, *12*, 1076−1078. (c) Jurczak, J.; Chmielewski, M. J.; Dydio, P.; Lichosyt, D.; Ulatowski, F.; Zieliński, T. *Pure Appl. Chem.* **2011**, *83*, 1543−1554. (d) Dydio, P.; Lichosyt, D.; Zieliński, T.; Jurczak, J. *Chem.-Eur. J.* **2012**, *18*, 13686−13701.

(17) (a) van Leeuwen, P. W. N. M.; Claver, C. *Rhodium Catalyzed Hydroformylation*; Kluwer Academic Publishers: Dordrecht, 2000. (b) Franke, R.; Selent, D.; Börner, A. *Chem. Rev.* **2012**, *112*, 5675−5732. (c) Breit, B.; Seiche, W. *Synthesis* **2001**, *2001*, 1−36.

(18) For regioselective hydroformylation of unfunctionalized internal alkenes, see: (a) Kuil, M.; Soltner, T.; van Leeuwen, P. W. N. M.; Reek, J. N. H. *J. Am. Chem. Soc.* **2006**, *128*, 11344−11345. For regio- and enantioselective hydroformylation of unfunctionalized internal alkenes, see: (b) Bellini, R.; Chikkali, S. H.; Berthon-Gelloz, G.; Reek, J. N. H. *Angew. Chem., Int. Ed.* **2011**, *50*, 7342−7345. (c) Gadzikwa, T.; Bellini, R.; Dekker, H. L.; Reek, J. N. H. *J. Am. Chem. Soc.* **2012**, *134*, 2860−2863. (d) Noonan, G. M.; Fuentes, J. A.; Cobley, C. J.; Clarke, M. L. *Angew. Chem., Int. Ed.* **2012**, *51*, 2477−2480.

(19) For regioselective hydroformylation of alkenes, using reversible covalent bonding of catalytic ligand-like directing groups, see: (a) Grünanger, C. U.; Breit, B. *Angew. Chem., Int. Ed.* **2008**, *47*, 7346−7349. (b) Grünanger, C. U.; Breit, B. *Angew. Chem., Int. Ed.* **2010**, *49*, 967−970. (c) Lightburn, T. E.; Dombrowski, M. T.; Tan, K. L. *J. Am. Chem. Soc.* **2008**, *130*, 9210−9211. (d) Worthy, A. D.; Gagnon, M. M.; Dombrowski, M. T.; Tan, K. L. *Org. Lett.* **2009**, *11*, 2764−2767. (e) Sun, X.; Frimpong, K.; Tan, K. L. *J. Am. Chem. Soc.* **2010**, *132*, 11841−11843. (f) Lightburn, T. E.; De Paolis, O. A.; Cheng, K. H.; Tan, K. L. *Org. Lett.* **2011**, *13*, 2686−2689. For a review on removable directing groups in organic synthesis and catalysis, see: (g) Rousseau, G.; Breit, B. *Angew. Chem., Int. Ed.* **2011**, *50*, 2450−2494 and references therein.

(20) Preliminary results of this study have been communicated: (a) Dydio, P.; Dzik, W. I.; Lutz, M.; de Bruin, B.; Reek, J. H. N. *Angew. Chem., Int. Ed.* **2011**, *50*, 396−400. For recent application of ligand L3 in β-selectivity hydroformylation of vinyl arenes, see: (b) Dydio, P.; Reek, J. H. N. *Angew. Chem., Int. Ed.* **2013**, *52*, 3878−3882.

(21) For low-temperature NMR studies of a mixture of eq−eq and eq−ax complexes, see: (a) Molina, D. A. C.; Casey, C. P.; Müller, I.; Nozaki, K.; Jäkel, C. *Organometallics* **2010**, *29*, 3362−3367. (b) Gual, A.; Godard, C.; Castillon, S.; Claver, C. *Adv. Synth. Catal.* **2010**, *352*, 463−477.

(22) van der Veen, L. A.; Keeven, P. H.; Schoemaker, G. C.; Reek, J. N. H.; Kamer, P. C. J.; van Leeuwen, P. W. N. M.; Lutz, M.; Spek, A. L. *Organometallics* **2000**, *19*, 872−883.

(23) For high-pressure IR studies, see: (a) van der Veen, L. A.; Boele, M. D. K.; Bregman, F. R.; Kamer, P. C. J.; van Leeuwen, P.W. N. M.; Goubitz, K.; Fraanje, J.; Schenk, H.; Bo, C. *J. Am. Chem. Soc.* **1998**, *120*, 11616−11626. (b) Kamer, P. C. J.; van Rooy, A.; Schoemaker, G. C.; van Leeuwen, P. W. N. M. *Coord. Chem. Rev.* **2004**, *248*, 2409−2424. (c) Kubis, C.; Ludwig, R.; Sawall, M.; Neymeyr, K.; Borner, A.; Wiese, K. D.; Hess, D.; Franke, R.; Selent, D. *ChemCatChem* **2010**, *2*, 287−295. (d) Diebolt, O.; van Leeuwen, P. W. N. M.; Kamer, P. C. J. *ACS Catal.* **2012**, *2*, 2357−2370.

(24) For details, see the Supporting Information.

(25) For the description of effective concentrations and of multivalency in supramolecular chemistry, see: Mulder, A.; Huskens, J.; Reinhoudt, D. N. *Org. Biomol. Chem.* **2004**, *2*, 3409−3424.

(26) Blackmond, D. G. *Angew. Chem., Int. Ed.* **2005**, *44*, 4302−4320.

(27) Copeland, R. A. *Enzymes: A Practical Introduction to Structure, Mechanism, and Data Analysis*; Wiley-VCH: New York, 2000.

(28) The effective concentration for substrate **8a** bound to the DIM pocket of the catalyst can be roughly estimated: (i) for the initial concentrations used and the association constant of $K_a > 10^5$ M^{-1}, the DIM pocket is nearly fully occupied by the substrate (>99.995%); (ii) the maximal distance between the Rh center and the alkene in the supramolecular complexes is about 15 Å; thus the "probing volume" is about 1.7×10^{-24} dm^3, which translates to the effective concentration $C_{eff} \approx 0.9$ M. With this rough estimate, one can understand that the nonbound substrate present in 0.2 M will considerably compete with the bound substrate. For comparison, for substrate **2a**, with the maximal Rh–alkene distance of 8Å, the effective concentration is estimated to $C_{eff} \approx 6$ M, which is substantially higher than the actual alkene concentration in solution (0.2 M), hence allowing for the effective competition. For a detailed discussion on the influence of the effective concentrations, see ref 25.

(29) Horiuchi, T.; Shirakawa, E.; Nozaki, K.; Takaya, H. *Organometallics* **1997**, *16*, 2981−2986.

(30) We started a search for possible conformations of the substrate–catalyst complex for both eq−eq and eq−ax coordination geometries, using a simplified model with a ligand in which the 4 phenyl rings were removed from the phosphine. Subsequently, the structures lowest in energy were supplemented with the phenyl rings and optimized again. (The geometries with much higher energies, >16 kJ mol^{-1}, were omitted.) For full computational details, see the Supporting Information.

(31) Despite many attempts, we were not able to find a transition state for the formation of the branched alkyl complex from this substrate–catalyst complex conformer.

(32) The complex structure is distorted from the ideal coordination geometry (a trigonal bipyramid or a square pyramid) due to the geometrical constrains imposed by the ligand and by the substrate bound to the phosphorus ligand (the virtually tridentate **L1−2a** ligand). Consequently, the two axial positions occupied by the hydride and CO are electronically different. Therefore, changing their positions leads to a complex with different energy, and also modifies the coordination geometry around the rhodium center. As indicated by the change of the τ parameter value from 0.39 to 0.27, for geometries **I** and **IV**, respectively, the inversion of the CO and H ligands pushes the geometry of the metal center to a structure closer to a square pyramid and results in its destabilization. (The τ value indicates the idealized square pyramid with τ = 0, and the trigonal bipyramid with τ = 1). For the description of the τ parameter, see: Addison, A. W.; Rao, T. N.; Reedijk, J.; van Rijn, J.; Verschoor, G. C. *J. Chem. Soc., Dalton Trans.* **1984**, 1349−1356.

(33) The isomerization of the internal double bond to the chain terminus, followed by its hydroformylation, gives access to linear products, see: (a) van der Veen, L. A.; Kamer, P. C. J.; van Leeuwen, P. W. N. M. *Angew. Chem., Int. Ed.* **1999**, *38*, 336−338. (b) Klein, H.; Jackstell, R.; Wiese, K.-D.; Borgmann, C.; Beller, M. *Angew. Chem., Int. Ed.* **2001**, *40*, 3408−3411. (c) Seayad, A.; Ahmed, M.; Klein, H.; Jackstell, R.; Gross, T.; Beller, M. *Science* **2002**, *297*, 1676−1678. (d) Bronger, R. P. J; Kamer, P. C. J.; van Leeuwen, P. W. N. M. *Organometallics* **2003**, *22*, 5358−5369. (e) Yu, S.; Chie, Y.-M.; Guan, Z.-h.; Zhang, X. *Org. Lett.* **2008**, *10*, 3469−3472. (f) Selent, D.; Franke,

R.; Kubis, C.; Spannenberg, A.; Baumann, W.; Kreidler, B.; Börner, A. *Organometallics* **2011**, *30*, 4509−4514.

(34) (a) van der Veen, L. A.; Boele, M. D. K.; Bregman, F. R.; Kamer, P. C. J.; van Leeuwen, P. W. N. M.; Goubitz, K.; Fraanje, J.; Schenk, H.; Bo, C. *J. Am. Chem. Soc.* **1998**, *120*, 11616−11626. (b) Casey, C. P.; Paulsen, E. L.; Buettenmueller, E. W.; Proft, B. R.; Petrovich, L. M.; Matter, B. A.; Powell, D. R. *J. Am. Chem. Soc.* **1997**, *119*, 11817− 11825.

(35) (a) van Leeuwen, P. W. N. M.; Kamer, P. C. J.; Claver, C.; Pàmies, O.; Diéguez, M. *Chem. Rev.* **2011**, *111*, 2077−2118. (b) Gual, A.; Godard, C.; Castillón, S.; Claver, C. *Tetrahedron: Asymmetry* **2010**, *21*, 1135−1146 and references therein.

(36) Although both ligand **L3** and the aldehyde products are chiral, there was no enantioselectivity observed in these reactions.

(37) Breit and co-workers reported selective hydroformylation of (Z)-pent-3-enoic acid, with relative regioselectivity of 18.1:1; see ref 11.